

# Corneal Curvature: the Influence of Corneal Accommodation and Biomechanics on Corneal Shape

Henry B. Wallace<sup>1</sup>, James McKelvie<sup>1</sup>, Colin R. Green<sup>1</sup>, and Stuti L. Misra<sup>1</sup>

<sup>1</sup> Department of Ophthalmology, Faculty of Medical and Health Sciences, New Zealand National Eye Centre, University of Auckland, Auckland, New Zealand

**Correspondence:** Stuti L. Misra, Department of Ophthalmology, Private Bag 92019, University of Auckland, Auckland, New Zealand. e-mail: s.misra@auckland.ac.nz

**Received:** 2 November 2018

**Accepted:** 11 May 2019

**Published:** 8 July 2019

**Keywords:** biomechanics; ocular accommodation; cornea; optics

**Citation:** Wallace HB, McKelvie J, Green CR, Misra SL. Corneal curvature: the influence of corneal accommodation and biomechanics on corneal shape. *Trans Vis Sci Tech.* 2019;8(4):5, <https://doi.org/10.1167/tvst.8.4.5>

Copyright 2019 The Authors

**Purpose:** Variation in the presence and magnitude of corneal conformational changes during accommodation may predict postoperative ectasia following refractive surgery and assist in the early diagnosis of corneal ectatic disorders. The current study aimed to establish a baseline for corneal refractive changes during ocular accommodation and to clarify the role of biomechanical factors in predicting these changes in a population without corneal pathology.

**Methods:** GALILEI G2 corneal tomography was assessed in 63 participants in both the accommodated and unaccommodated states. Four diopters (D) of physiological accommodation were induced using near-acuity calibrated words viewed through an externally mounted beam splitter mounted on a three-dimensional-printed frame. Corneal biomechanical characteristics were assessed with the CorVis-ST instrument, and statistical analysis was completed in R software.

**Results:** Anterior chamber depth was reduced by  $0.10 \pm 0.07$  mm with accommodation ( $P < 0.01$ ). Areas of statistically significant change in corneal curvatures were seen in all participants with accommodation. Mean anterior instantaneous corneal power increased in the superior-nasal periphery (0.1 D, 95% confidence interval [CI] = 0.05–0.2 D) and decreased in the inferior-temporal periphery (0.1 D, 95% CI = –0.05 to –0.15 D). Corneal stiffness and the corneal deformation amplitude ratio predicted peripheral corneal curvature changes with accommodation ( $P < 0.05$ ).

**Conclusion:** Corneal conformational changes occur during accommodation in normal subjects. Further studies are required to assess the magnitude of corneal changes during accommodation in patients with corneal ectasia.

**Translational Relevance:** An externally mounted beam splitter can be used to modify the visual target presented by clinical ocular imaging instruments. Corneal conformational changes during accommodation may be useful in the diagnosis of corneal ectasia.

## Introduction

Corneal conformation can be described by the combination of corneal curvature, height (elevation), and pachymetry measurements. As the primary refractive element in the eye, any change in corneal conformation associated with accommodation may contribute to accommodative power. For example, a 0.7-mm reduction in anterior corneal radius during accommodation would induce 4 diopters (D) of myopic shift.<sup>1</sup> Corneal changes of this magnitude

are unlikely; however, the ciliary muscle lies in close proximity to the cornea and some of its tendons insert directly into the cornea.<sup>2</sup> Contraction of the ciliary muscle induces corneal conformational changes in avian species,<sup>3</sup> and it has been suggested that similar conformational changes may occur in the peripheral human cornea.<sup>4–6</sup> The human cornea typically retains a remarkably stable refractive power throughout life except in cases of corneal ectasia. It is possible that increased corneal conformational changes during physiological accommodation may be useful to predict the likelihood of corneal ectasia in refractive

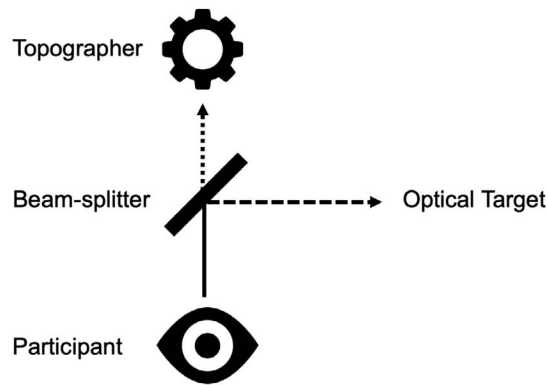


**Figure 1.** Ray diagram of optical system used to control accommodation and measure corneal tomography. The optical target was set at one of two distances: 0.25 m for the accommodated condition and 6 m for the unaccommodated condition.

surgery patients and assist in the early diagnosis of ectatic disorders of the cornea, such as keratoconus.

Studies of the relationship between ocular accommodation and corneal curvature have become progressively sophisticated as anterior segment imaging and quantification of refractive power has become increasingly sensitive. Early studies utilized keratometers,<sup>7-9</sup> which were superseded by studies using videokeratoscopy,<sup>10,11</sup> Placido-disc topographers,<sup>4,11,12</sup> and eventually Scheimpflug<sup>6,13</sup> or Dual-Scheimpflug tomographers.<sup>5</sup> These studies have produced conflicting reports on the presence, magnitude, and direction of corneal changes with accommodation<sup>4,6,9,10</sup>; however, the majority concluded that corneal conformation does not significantly change during accommodation.<sup>5,12-15</sup> Furthermore, the magnitude of total refractive change during accommodation appears to be equivalent to the lenticular refractive change,<sup>16</sup> and anterior segment ultrasound biomicroscopy images can be accurately aligned using the cornea as a fixed reference point for images captured in various accommodative states.<sup>17</sup>

The biomechanical properties of the cornea affect corneal curvature, strength, and conformability.<sup>18</sup> There are currently no agreed gold standard clinical investigations to characterize corneal biomechanics, but the surrogate markers of corneal stiffness obtained by the CorVis ST (Oculus, Wetzlar, Germany) instrument provide arguably the best noninvasive in vivo assessment of these parameters. The CorVis ST instrument assesses the dynamic corneal response to a 60-mmHg, 3.05-mm-diameter, air puff using ultra-high-speed Scheimpflug imaging.<sup>19</sup> This allows the visualization and analysis of various

biomechanical parameters. Recent software updates to CorVis ST have introduced novel corneal stiffness parameters that serve as biomarkers for more flexible corneas and potentially for conformational changes during ocular accommodation.<sup>19</sup>

The current study demonstrates a novel method for inducing physiological accommodation, and corneal tomography is assessed to a peripheral radius of 5 mm. The current study is the first to analyze the effect of prospectively measured corneal biomechanical parameters on the presence and magnitude of corneal conformational changes during accommodation.

## Methods

### Study Design

The present study was a crossover study with all participants tested in the accommodated and nonaccommodated states for comparison. The study was conducted in accordance with the Declaration of Helsinki, with formal approval obtained from the Health and Disability Ethics Committee of New Zealand (reference: 16/CEN/132). The study was registered in the Australian New Zealand Clinical Trials Registry under registration number ACTRN12616001593426. All participants were aged 18 years or older and provided written consent prior to participation. Exclusion criteria were uncorrected visual acuity less than logMAR 0.3 (Snellen 6/12), pre-existing ocular pathology or previous ocular surgery, contact lens use, strabismus, and previous ocular trauma. Participants were recruited using posters placed around The University of Auckland Grafton Campus. All participation was on a voluntary basis, and participants were not remunerated in any way.

Power analysis using G\*Power for Mac (version 3.1.9.2; Heinrich-Heine-Universität Düsseldorf, Düsseldorf, Germany) indicated that a sample size of over 60 participants would produce >90% power to detect changes in corneal curvature of a magnitude demonstrated in other studies with *t*-tests.<sup>4,6</sup>

### Machine Assembly

Ocular accommodation was controlled by the presentation of optical targets at different distances from participants (Fig. 1). The addition of a beam splitter to the optical system of GALILEI G2 was required to allow simultaneous tomography measurements and the presentation of these varied optical

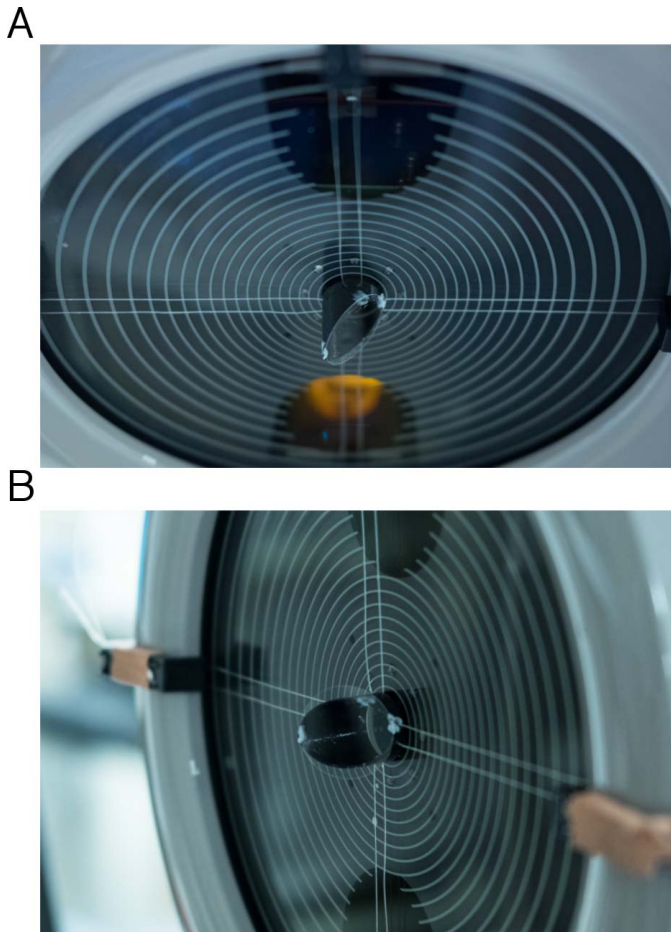


**Figure 2.** Photographs of the Galilei G2 with the beam splitter attached. (A) View from above and in front of the Galilei G2; (B) view from right hand side.

targets. To avoid major modifications to the existing tomographer, which was in current clinical use at the time of the study, a beam splitter angled at  $45^\circ$  to the optical axis was mounted externally with a custom three-dimensional (3D)-printed polylactic acid housing (Fig. 2). The beam splitter itself was a transparent, 2-cm-diameter circular microscope slide cover.

The beam splitter housing was suspended within the central Placido ring of GALILEI G2 by fine nylon cord attached to the tomographer using 3D-printed polylactic acid fasteners (Fig. 3). The fasteners allowed rapid, consistent addition and removal of the beam splitter from the optical system. The fasteners also avoided the use of adhesives and allowed the beam splitter housing to be placed in contact with the Placido disk of GALILEI G2, guaranteeing parallel alignment in the plane of the Placido disk. The fasteners were attached to the perimeter of the measurement head and were consistently aligned using drawn markings on GALILEI G2. A small amount of ocular elevation was required to read the target words above the blue light used by GALILEI G2 to acquire Scheimpflug images (Fig. 4).

### Examination Technique

All measurements were obtained from right eyes in the University of Auckland Ocular Imaging Unit by a single examiner. All participants had corneal tomography measured in the accommodated and unaccommodated states with GALILEI G2. The dynamic corneal response was measured with the CorVis ST (Oculus, Wetzlar, Germany) instrument, refraction

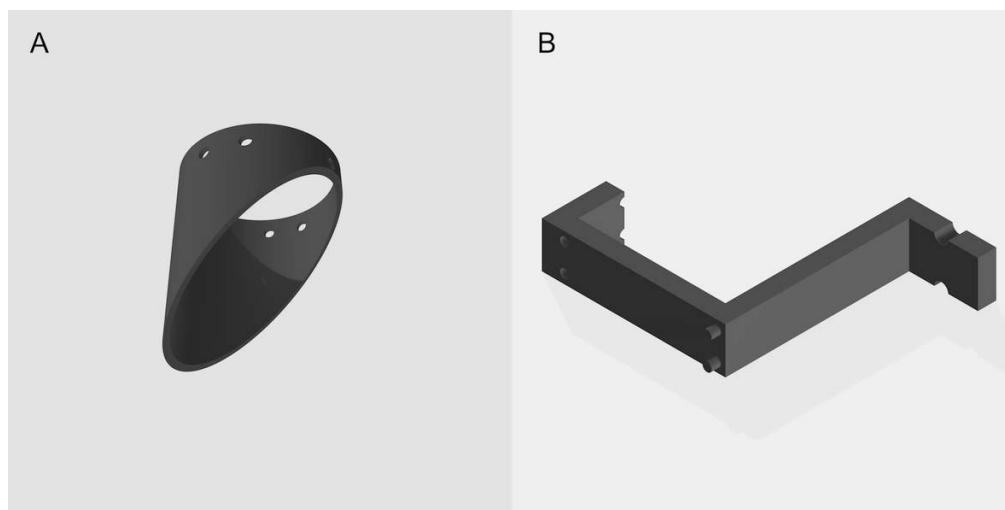


**Figure 3.** Computer models of the beam splitter housing and fasteners. *Left*, 3D-printed mount for beam splitter. *Right*, 3D-printed fastener for attaching and removing the mount from the GALILEI G2. The hole in the design enables the nylon cord to secure and precisely position the components.

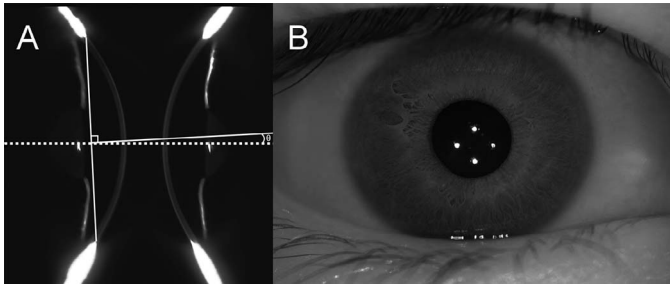


**Figure 4.** Galilei G2 Alignment with a participant viewing external targets. All images were captured during the same examination. (A) Alignment of the cornea in a Scheimpflug image. Dotted line, tomographer axis. The visual axis was approximated by a line orthogonal to that connecting the superior and inferior limbus, and angle  $\theta$  approximates gaze elevation (mean =  $0.67^\circ$ ); (B) Alignment of Purkinje images of the Galilei G2 targeting system relative to the pupil. There is slight horizontal displacement due to angle  $\kappa$  and vertical displacement because ocular elevation was required to view the visual target (for near and distance).

was measured with the ARKM-200 Autokeratometer (Takagi Seiko Co., Ltd, Nagano-ken, Japan), and the near point of accommodation assessed with a Royal Air Forces Ruler.

The order of the accommodated and unaccommodated (control) conditions was randomized. In the accommodated condition, 4 D of accommodation were induced by an accommodative target viewed 0.25 m anterior to the spectacle plane. The accommodative target consisted of four-letter words, in black Times New Roman font on a white background, to mimic standard near acuity vision charts used in New Zealand. One hundred words were randomly selected from a list of four-letter words and displayed on separate Microsoft PowerPoint (Redmond, WA) slides programmed to change every 1 second. The text was then digitally mirror inverted and the PowerPoint presentation exported as a video file. The video was looped on a smartphone screen using the VLC video player application (VideoLAN organization, multinational). The final text size on the smartphone screen was scaled to display at a size to match the threshold of N6 acuity. The unaccommodated control condition used a target viewed at 6 m from the spectacle plane. The control target consisted of the same four-letter words displayed on the same smartphone screen, using the same method. The control target words were displayed using Sloan font, in black on a white background, at a size equivalent to logMAR 0.3 (Snellen 6/12).<sup>20</sup>

Six corneal topography examinations of the right eye were captured in both the accommodated and unaccommodated states. Between the accommodated

and unaccommodated conditions, there was a minimum 5-minute rest period. Measurements were obtained in scotopic conditions with the contralateral (left) eye covered with an opaque noncontact occluder to control convergence.

## Data Evaluation

The GALILEI G2 can export 18,001 data points at a 0.1-mm resolution for corneal height, curvature, and pachymetry data. These raw data were used for statistical analysis. Measurements were only kept if reported to be of adequate quality by the GALILEI software (version 6.0.2). Corneal height data, which are the distance from the measurement face of the tomographer to the cornea, were affected by small translations of the tomographer between the 12 independent measurements of each subject (accommodated,  $n = 6$ ; unaccommodated,  $n = 6$ ). These translations were assumed not to affect the relative difference between corneal height points. Translations were compensated for in each examination by subtracting the arithmetic mean corneal height of the from each of the data points.

Tomographic assessments with GALILEI are spatially corrected for comparison by using a patented iris detection algorithm.<sup>5</sup> However, on initial screening of the data, it was apparent that each scan had subtly differing amounts of cyclorotation.<sup>13</sup> A method for correcting these spatial errors has been described, and this was encoded in the open source programming language R.<sup>21</sup> The error associated with compiling multiple measurements can be quantified by the sum of squared differences from the plane  $x + y + z = 0$ . Following the application of this algorithm, the arithmetic mean reduction in the sum of squared differences was 57%.

## Statistical Analyses

Statistical analysis was conducted in the R statistical analysis package (R Foundation for Statistical Computing, Vienna, Austria). Intraobserver repeatability for GALILEI G2 was assessed with the 3D-printed mount in place using the six measurements taken in the unaccommodated state for each participant.<sup>22,23</sup> Repeatability was quantified using the within-subject standard deviation ( $S_w$ ), precision, test-retest variability (repeatability), coefficient of variation (CoV), and intraclass correlation (ICC). Precision was calculated as  $1.96 \times S_w$ , because for 95% of observations, the difference between a subject's measurement and the true value would be

expected to be less than  $1.96 \times S_w$ . Test-retest variability, or repeatability, was calculated as  $2.77 \times S_w$ . The within-subject CoV was calculated as the  $S_w$  divided by the overall mean and expressed as a percentage. The ICC is defined as the ratio of the between-subjects' variance to the sum of the combined within-subjects and between-subjects' variance. The ICC values range from 0 to 1, with 1 indicating perfect agreement.

The Bland-Altman method was used to assess the effect of the 3D-printed mount and ocular elevation on GALILEI G2 measurements, compared to measurements in the same eye of the same single participant.<sup>24</sup> For the Bland-Altman analysis, the same participant was measured five times in each of the following measurement conditions: neutral eye position with no device modifications, neutral eye position with 3D-printed mount in place, and elevated eye (to view study target) with 3D-printed mount in place. Significant differences were identified with a one-sample *t*-test with the test value equal to zero.<sup>22,24</sup> The 95% limits of agreement (mean difference  $\pm 1.96 \times$  standard deviation) were used to define the confidence interval within which most differences between measurements from the pairwise comparisons will occur.<sup>22,24</sup>

Arithmetic means of each data point were calculated for the six scans in the accommodated and unaccommodated conditions, for each parameter, for each participant. The difference between the accommodated and unaccommodated conditions were calculated by subtracting the accommodated value from the unaccommodated value. These data were interpolated onto a  $100 \times 100$  matrix to generate individual contour plots (Fig. 5A).<sup>25</sup> Statistically significant changes were detected with paired *t*-tests by comparing the series of six scans in the accommodated and unaccommodated conditions. The *P* values of the tests were extracted and interpolated onto a  $100 \times 100$  matrix to create statistical significance contour plots (Fig. 5B).<sup>25</sup> The cornea was split into 12 sectors to statistically assess the distribution of changes. These 12 sectors comprised of 3 zones (Central [ $r \leq 1.5$  mm], Paracentral [ $1.5 > r \geq 3.5$  mm], and Peripheral [ $3.5 > r \geq 5$  mm]) in each of four quadrants (Upper, Lower, Nasal [left], and Temporal [right]). The percentage of data points with a *P* value  $< 0.05$  were calculated in each sector and compared with proportion tests to assess statistical differences between sectors.<sup>26</sup> Mean corneal changes across the entire study population were assessed by taking the arithmetic mean change at each data point. Statisti-

cally significant mean changes were identified with one-sample *t*-tests with the test value equal to zero.

Multiple regression analysis was used to determine if corneal biomechanical parameters predict corneal changes occurring during accommodation. Total corneal changes were estimated using the sum of squared displacement for each data point from the plane  $x + y + z = 0$ . Biomechanical parameters for regression were extracted from CorVis ST. To avoid including highly collinear variables in the analysis, variables with the largest mean absolute correlation from pairs of variables with correlation coefficients  $> 0.7$  were removed from the analysis. The remaining variables that had been previously shown to be associated with corneal stiffness were included in the analysis with the additional variables of ethnicity, age, sex, and percentage anterior chamber depth (ACD) change.<sup>19</sup>

## Results

Sixty-three right eyes of 63 participants were recruited for and included in the current crossover study. The arithmetic mean age of participants ( $\pm$  standard deviation) was  $24.2 \pm 4.60$  years. Four participants (6%) were over the age of 30. The mean maximum accommodative power was  $9.1 \pm 1.44$  D, as measured by Royal Air Forces ruler. The mean objective spherical equivalent refraction was  $0.2 \pm 0.6$  D. The mean biometry corrected intraocular pressure (bIOP) was  $13.4 \pm 2.0$  mmHg, and the mean pachymetry was  $539 \pm 29$   $\mu$ m.

The results of the repeatability analysis are summarized in Table 1. There was good or excellent measurement repeatability (ICC,  $> 0.7$ ) for all parameters except posterior corneal height and peripheral pachymetry. The lowest ICC values occurred for the posterior height data (mean ICC = 0.323). Peripheral pachymetry showed poor repeatability (ICC = 0.406) compared to central (ICC = 0.994) and paracentral pachymetry (0.942).

The results of the Bland-Altman analysis for measurement agreement in different states of optical system modification are summarized in Figure 6 and Table 2. The addition of the beam splitter and gaze elevation had a minimal effect on anterior corneal height measurements (mean difference = 0 mm), and the 95% limits of agreement were reduced by over 50% from within 0.02 mm to within 0.01 mm when the data were passed through the spatial correction algorithm. The addition of the beam splitter and gaze elevation caused statistically significant fixed bias for

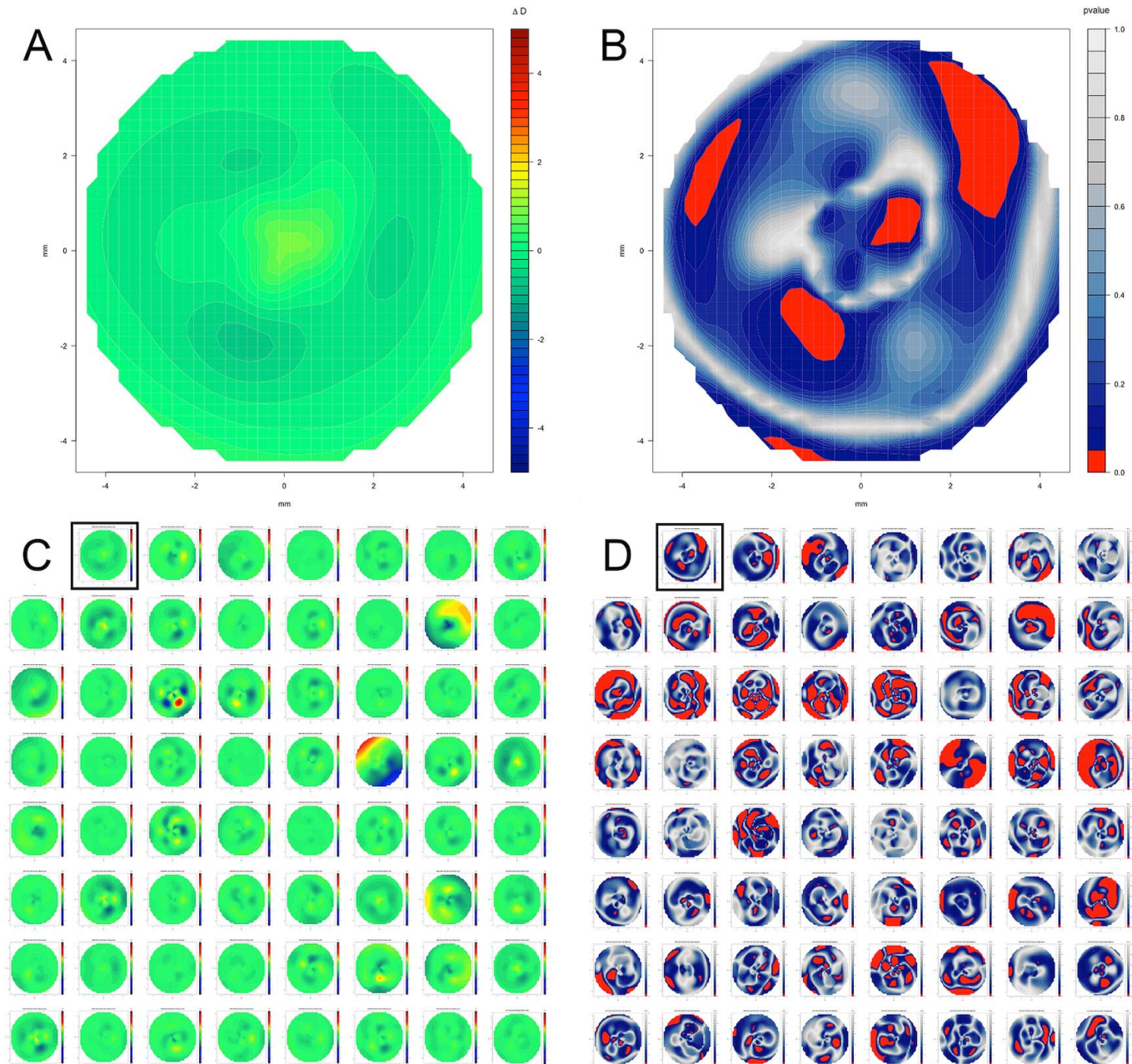


**Figure 5.** Anterior instantaneous corneal curvature changes for each of 63 participants with accommodation. (A) Anterior instantaneous corneal curvature changes with accommodation for a single participant. The color scale is from +5 D (red) to -5 D (navy blue). Spring green indicates no change. (B) Areas of significant ( $P < 0.05$ ) anterior curvature change with accommodation are displayed in red, for a single participant. Darker blue regions indicate changes approaching statistical significance. (C) Anterior instantaneous corneal curvature changes with accommodation for all participants. Plots are ordered according to participants' unique and random hexadecimal identifier. (D) Areas of statistically significant anterior instantaneous corneal curvature change with accommodation, for each participant. The plots are arranged in the same order as (A) to facilitate comparison.

pachymetry and anterior axial curvature measurements ( $P < 0.01$ ). For pachymetry measurements, the largest mean bias occurred during elevation with the beam splitter in place ( $1.38 \mu\text{m}$ ,  $P < 0.01$ ). The largest mean bias occurred with only the addition of the

beam splitter for anterior axial curvature ( $0.14 \text{ D}$ ,  $P < 0.01$ ), and ocular elevation caused a statistically significant fixed bias for anterior instantaneous curvature measurements ( $0.41 \text{ D}$ ,  $P < 0.01$ ).

Arithmetic mean ACD reduced by  $-0.100$  (stan-

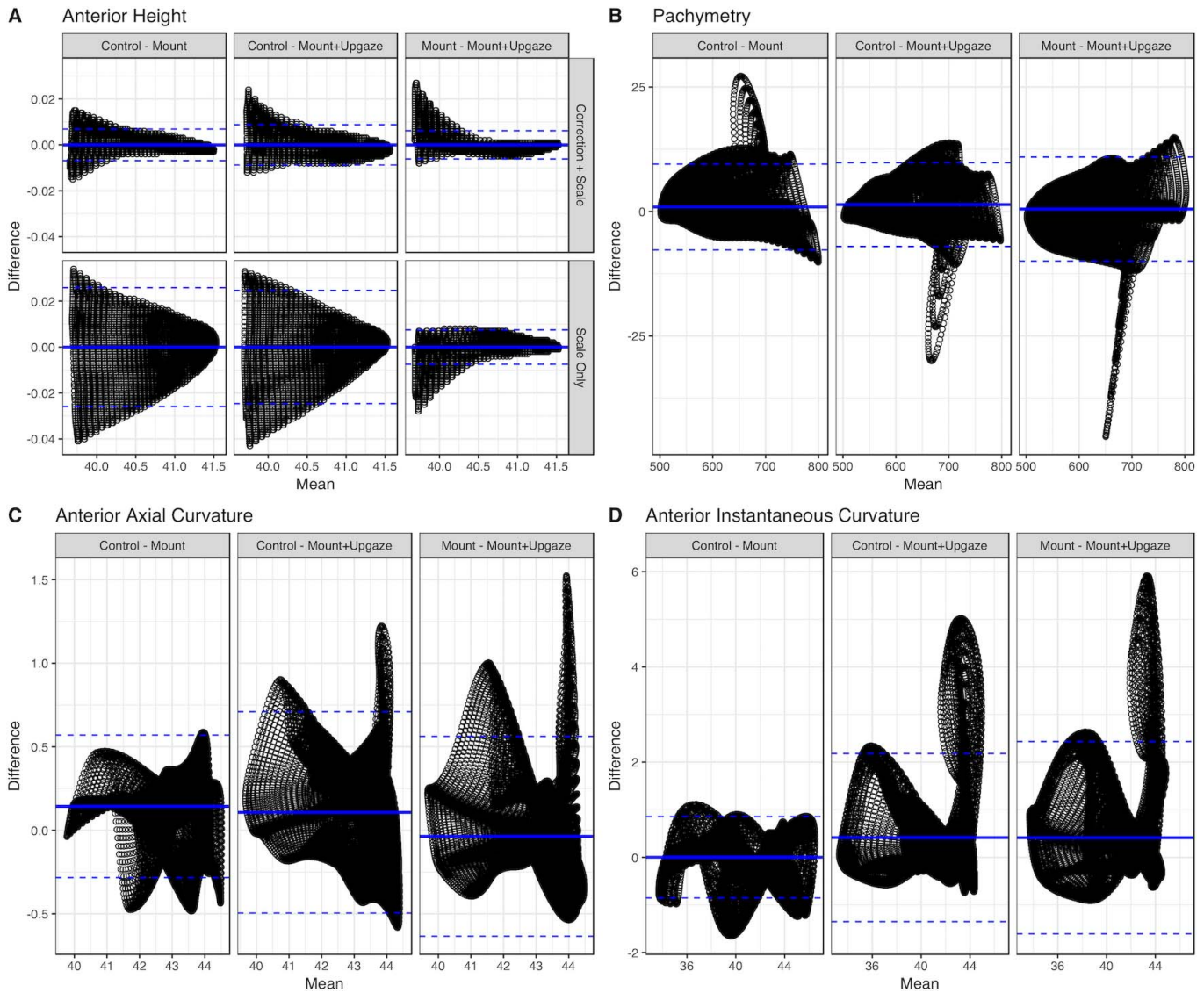


**Figure 6.** Bland-Altman plots for agreement between selected parameters for measurement-procedure modification pairs. The anterior height analysis is split into two facets to show the improvement in the 95% limits of agreement once the spatial correction algorithm was applied. Ant, anterior; CURV, curvature; solid *central line* represents mean of the difference between the two devices. *Dashed lines* represent 95% limits of agreement.

dard deviation = 0.073 mm) with accommodation ( $P < 0.01$ ). Changes in anterior instantaneous corneal curvature with accommodation are summarized for each participant in [Figure 5C](#). The corresponding areas of significant change are summarized in [Figure 5D](#). Individual anterior instantaneous curvature changes were typically within  $\pm 0.5$  D. The mean changes in anterior and posterior instantaneous curvatures with accommodation are displayed in [Figures 7A](#) and [7C](#), respectively. Anterior instantaneous curvature changes resulted in an increase of corneal power of approximately 0.1 D centrally and in

the superior nasal periphery. Corresponding decreases in corneal power occurred in the lower periphery and also in the nasal paracentral region. Significant changes were more commonly noted in the corneal periphery ([Fig. 7E](#)). Posterior instantaneous curvature changed less relative to anterior instantaneous curvature, with changes of less than 0.1 D peripherally, as well as in the lower paracentral area. Anterior and posterior axial curvatures for comparison to the instantaneous curvatures are displayed in [Figures 7B](#) and [7E](#). The distribution of axial curvature changes mirror the changes in instantaneous curvature;

**Table 1.** Intraobserver Repeatability Metrics for GALILEI G2 with the 3D-Printed Mount in Place<sup>a</sup>

Exam	Zone	Mean (mm)	SD (mm)	Sw SD (μm)	Prec. (μm)	Rep. (μm)	CoV	ICC
Anterior height	Central	41.58	0.156	2.66	5.21	7.36	0.006	0.999
Anterior height	Paracentral	41.185	0.158	0.59	1.15	1.62	0.001	1
Anterior height	Peripheral	40.351	0.169	3.33	6.52	9.22	0.008	0.999
Posterior height	Central	41.03	0.152	4.28	8.38	11.84	0.01	0.29
Posterior height	Paracentral	40.547	0.156	1.67	3.27	4.62	0.004	0.302
Posterior height	Peripheral	39.484	0.179	6.3	12.34	17.44	0.016	0.376
Pachymetry	Central	543	27	1	2	3	0.2	0.994
Pachymetry	Paracentral	588	28	2	4	5	0.315	0.942
Pachymetry	Peripheral	678	36	9	18	26	1.368	0.406
Axial-CURV-ANT	Central	43.1	1.7	0.411	0.806	1.139	0.953	0.852
Axial-CURV-ANT	Paracentral	42.5	1.3	0.188	0.369	0.522	0.443	0.944
Axial-CURV-ANT	Peripheral	42.2	1.3	0.148	0.289	0.409	0.349	0.975
Axial-CURV-POST	Central	-6.2	0.3	0.066	0.13	0.184	-1.068	0.895
Axial-CURV-POST	Paracentral	-6	0.2	0.034	0.067	0.094	-0.563	0.901
Axial-CURV-POST	Peripheral	-6	0.2	0.036	0.071	0.101	-0.61	0.835
INST-CURV-ANT	Central	42.8	1.5	0.281	0.551	0.779	0.657	0.894
INST-CURV-ANT	Paracentral	41.8	1.3	0.175	0.344	0.486	0.419	0.968
INST-CURV-ANT	Peripheral	42.1	1.3	0.146	0.286	0.405	0.347	0.977
INST-CURV-POST	Central	-6.1	0.2	0.043	0.085	0.119	-0.705	0.924
INST-CURV-POST	Paracentral	-5.9	0.2	0.057	0.112	0.158	-0.975	0.716
INST-CURV-POST	Peripheral	-6	0.2	0.055	0.107	0.152	-0.912	0.87

<sup>a</sup> ANT, anterior; CoV, coefficient of variation; CURV, curvature; INST, instantaneous; POST, posterior; Prec, Precision; Rep, repeatability.

however, the magnitude of the changes is smaller and the plots appear smoother overall.

The mean anterior height displacements with accommodation and the corresponding areas of statistically significant change for all participants are demonstrated in [Figures 8A](#) and [8B](#). The displacements were predominantly small (<1.5 μm), posterior, and peripheral. The lower central corneal sector had a high proportion of significant changes (24.5%), and the inferosuperior axis had more significant changes than the mediolateral axis. The mean pachymetry changes with accommodation and the corresponding areas of statistically significant change for all participants are demonstrated in [Figures 8C](#)

and [8D](#). There was central corneal thinning (0.5 μm) and peripheral corneal thickening (0.125–0.75 μm). The paracentral zone was largely unchanged. Fewer than 10% of pachymetry data points were significantly changed for each corneal sector, except the peripheral nasal sector.

Multiple linear regression showed that various corneal biomechanical factors were significantly associated with corneal conformational changes during accommodation ( $P < 0.05$ ). The model fits were, however, very poor for all parameters (adjusted  $R^2$  range = 0.035–0.169). [Table 3](#) demonstrates factors predicting anterior instantaneous corneal curvature change with accommodation. bIOP and 1-mm defor-

**Table 2.** Mean Differences between Selected Parameters for Measurement-Procedure Modification Pairs<sup>a</sup>

Comparison	Ant. Height	Pachymetry	Ant. Axial Curvature	Ant. Inst. Curvature
Control vs. mount	0	0.90**	0.14**	0
Control vs. mount + upgaze	0	1.38**	0.11**	0.42**
Mount vs. mount + upgaze	0	0.48**	-0.04**	0.41**

<sup>a</sup> \*\*,  $P < 0.01$ ; Ant, anterior; Inst, instantaneous.

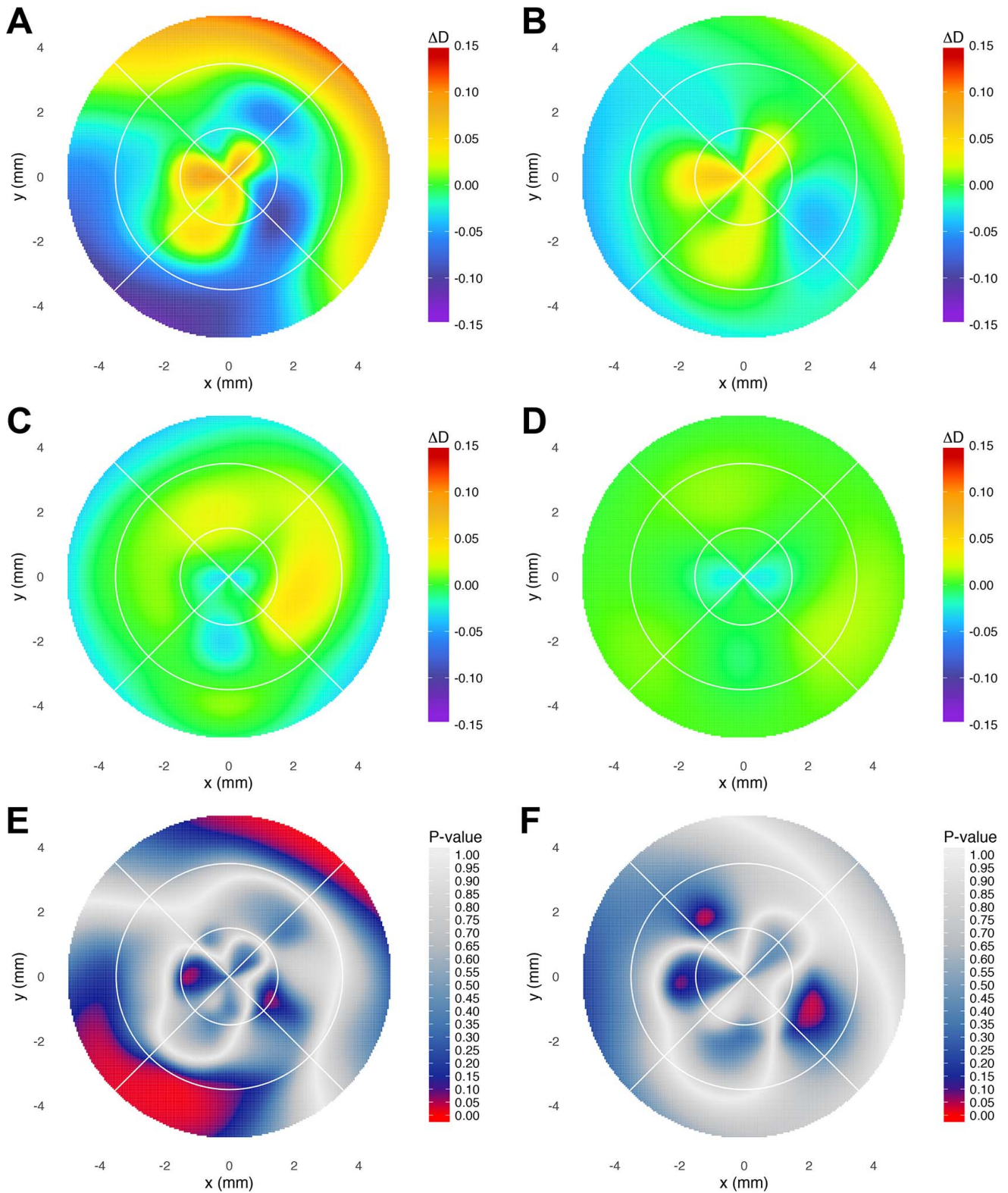


**Figure 7.** Mean anterior and posterior corneal curvature changes with accommodation. *White lines* define 12 corneal sectors derived from three zones (central [radius ( $r$ )  $\leq 1.5$  mm], paracentral [ $1.5 > r \geq 3.5$  mm], peripheral [ $3.5 > r \geq 5$  mm]) and four quadrants (*upper*, *lower*, *nasal* [*left*], *temporal* [*right*]). (A) Anterior instantaneous curvature; (B) anterior axial curvature; (C) posterior instantaneous curvature; (D) posterior axial curvature; (E) statistically significant regions of mean anterior instantaneous curvature change; (F) statistically significant regions of mean anterior axial curvature change.

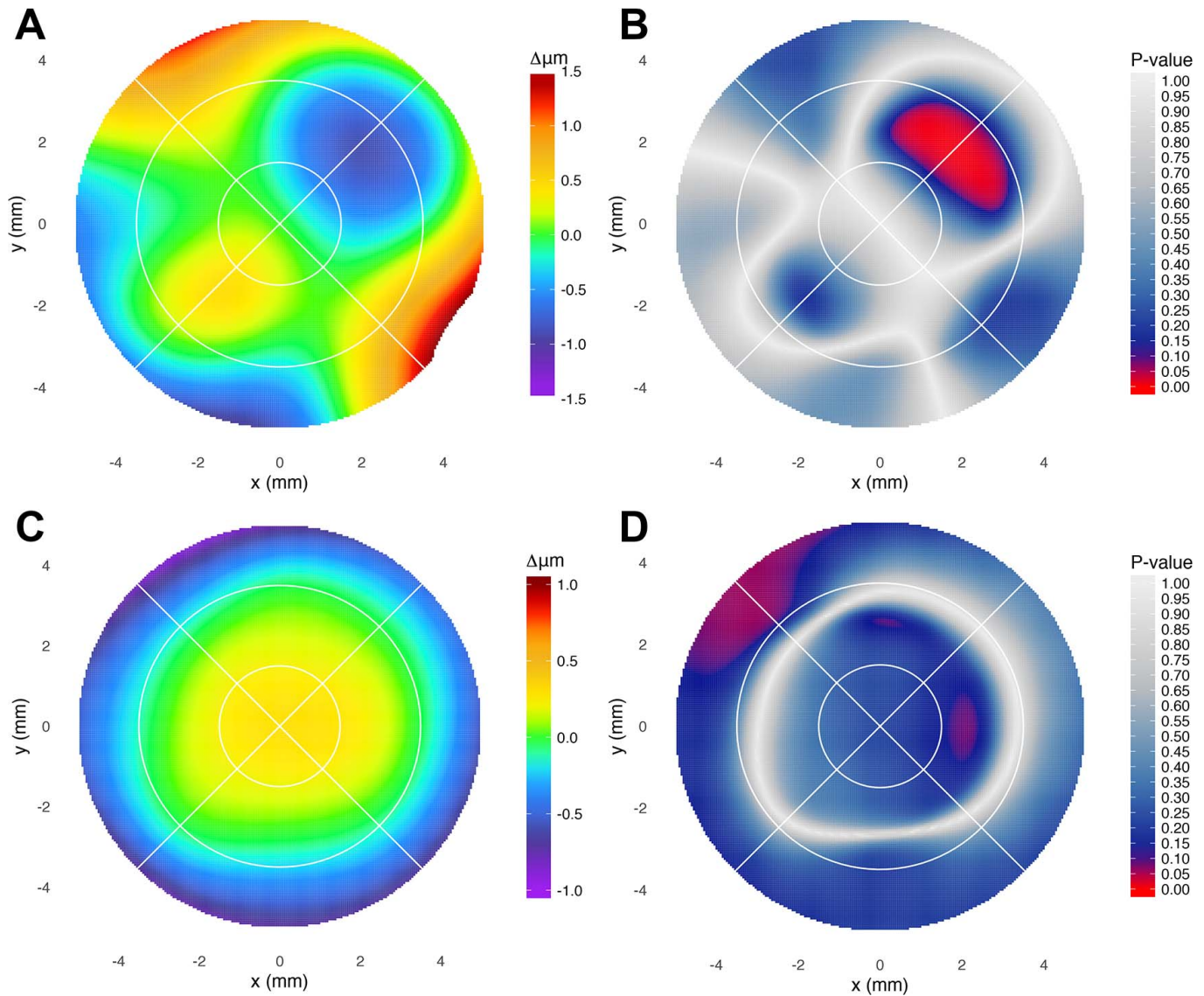


**Figure 8.** Anterior corneal height and pachymetry changes with accommodation. Corneal height is the distance between the corneal surface and the measuring tomographer. *White lines* define 12 corneal sectors derived from three zones (central [ $r \leq 1.5$  mm], paracentral [ $1.5 > r \geq 3.5$  mm], peripheral [ $3.5 > r \geq 5$  mm]) and four quadrants (upper, lower, nasal [left], temporal [right]). (A) Mean anterior corneal height change; (B) regions of statistically significant mean anterior height change; (C) mean corneal thickness change; (D) regions of statistically significant mean corneal thickness change.

mation amplitude (DA) ratio were negatively correlated with increased central corneal power, whereas Pacific ethnicity and male sex were positively correlated ( $P < 0.05$ ). Parameters negatively correlated with increased paracentral corneal power were percentage ACD change and peak distance, whereas male sex was positively correlated ( $P < 0.05$ ). Increased peripheral corneal power was negatively correlated with first applanation stiffness parameter (SP A1), 1-mm DA ratio, first applanation (A1) DA,

and percentage ACD change, whereas time of highest concavity was positively correlated ( $P < 0.05$ ).

## Discussion

The current study aimed to establish a baseline for corneal refractive changes during ocular accommodation and to clarify the role of biomechanical factors in predicting these changes in a population free from corneal pathology. The corneal tomography of 63

**Table 3.** Factors Predicting Anterior Corneal Curvature Change with Accommodation<sup>a</sup>

Variable	Central	Paracentral	Peripheral
(Intercept)	4218	11332	258
Pachymetry ( $\mu\text{m}$ )	-3	-1	6
bIOP (mmHg)	-86*	-38	54
SP A1	9	-9	-20*
DA Ratio (1 mm)	-2465*	-2095	-3542*
A1 DA (mm)	2266	660	-4610
A2 Velocity ( $\text{ms}^{-1}$ )	6	-202	1223
HC Time (ms)	175	-77	304*
Peak Distance (mm)	-224	-878*	-106
$\Delta$ ACD (%)	-2	-97.21**	-118***
Ethnicity (European)	67	-128	-547***
Ethnicity (Māori)	77	69	-371
Ethnicity (MiddleE)	98	-476 <sup>†</sup>	-857***
Ethnicity (Pacific)	508***	36	-509*
Age (Days)	0	0	0
Sex (Male)	196**	303**	7

<sup>a</sup> Values are the expected change in the sum of squared diopters of corneal power with every increase of 1 unit of the dependent variable, compared to the intercept variable; <sup>†</sup>,  $P < 0.075$ ; \*,  $P < 0.05$ ; \*\*,  $P < 0.01$ ; \*\*\*,  $P < 0.001$ .  $\Delta$ , change; A1, first applanation; A2, second applanation; bIOP, biometry corrected IOP; DA, deformation amplitude; HC, highest concavity; MiddleE, Middle Eastern; SPA1, stiffness parameter A1

normal participants were evaluated, and physiological accommodation was stimulated using a novel method allowing for the viewing of an external target viewed at 25 cm through an externally mounted beam splitter.

Statistically significant corneal curvature changes occurred in every participant with accommodation. These changes occurred significantly more often in the corneal periphery when compared to the central and paracentral corneal zones. The changes trended toward increased power in the superior cornea and decreased power in the inferior cornea. On average, 15% of the anterior central cornea significantly increased in refractive power up to a maximum of 0.1 D on analysis of both the axial and instantaneous curvatures. Posterior corneal changes were negligible for both axial and instantaneous curvatures. This is possibly due to the decreased sensitivity of the posterior corneal measurements, which are derived solely from the Scheimpflug images as opposed to the anterior curvatures that incorporate information

from Placido discs.<sup>27</sup> Given the minimal influence of the posterior corneal surface on overall refractive power, these small changes can be largely disregarded. Anterior corneal height and corneal pachymetry changes were also statistically significant but clinically insignificant.

Corneas with biomechanical factors indicating decreased stiffness were hypothesized to exhibit increased changes with accommodation.<sup>14</sup> The primary biomechanical factors of interest were bIOP and corneal thickness.<sup>19</sup> Lower intraocular pressure was associated with central corneal changes, likely due to decreased radially directed counter force against corneal movement.<sup>28</sup> Similarly, thinner corneas are known to have reduced stiffness, even when the collagen concentration is normal.<sup>29</sup> Although corneal thickness did not correlate with increased refractive changes, the first applanation corneal stiffness parameter was significantly associated with increased peripheral curvature changes.

Human corneal and lens tissue stiffens with age, and lens stiffening results in an inevitable reduction in accommodative amplitude.<sup>30,31</sup> In contrast, the muscular power of the ciliary muscle is maintained with age, despite a relative increase in nonfunctional connective tissue components.<sup>32,33</sup> Because of the interaction between accommodative amplitude, lens aging, corneal cross-linking, and ciliary muscle aging, the authors of the current study hypothesized that young adults would exhibit the largest corneal changes with accommodation.

An accommodative stimulus with polychromatic white light was used to maximize accommodation during assessment with a near target. Monochromatic light is a poor stimulus for accommodation because the human eye has difficulty with precisely adjusting focus on objects illuminated with monochromatic light.<sup>34</sup> Second, point sources of light fail to produce a strong stimulus for accommodation. Optical movements of at least 6 minutes of arc are sufficient to stimulate a change in accommodative amplitude during fixation.<sup>34</sup> Many recent studies assessing accommodative corneal conformational changes have used a monochromatic point light as an accommodative stimulus.<sup>5,6,13</sup> This design flaw was avoided in the current study through the use of a constantly changing target illuminated by white light.

The elevation of gaze away from the measurement plane of the tomographer is the major limitation of the current study. Even with the central target light of GALILEI G2 inactivated, it was not possible to gain enough contrast for participants to read the target

words projected inside the annulus of 700-nm blue light, which GALILEI G2 uses to acquire Scheimpflug images. Consequently, the target had to be elevated. However, minimal ocular elevation (approximately  $0.67^\circ$ ) was required to view the elevated target, and Bland-Altman agreement analysis demonstrated clinically insignificant effects on both anterior height and pachymetry measurements. Additionally, the current study was concerned with demonstrating a difference in individuals between the accommodated and unaccommodated conditions, so any effect of the beam splitter, gaze elevation, or convergence was uniform throughout the experiment, and the demonstrated differences are the result of corneal changes with accommodation.

The use of spatial correction for anterior height data is a strength of the current study. The current study has shown that this algorithm is useful in combining data from multiple scans for GALILEI G2, although it was initially proposed for use with older videokeratographers. Statistically significant corneal changes with accommodation persisted after digital correction of the corneal elevation data.<sup>21</sup>

The hypothesized clinical applications of the current study centered around whether corneal accommodation could be a marker of corneal ectasia risk, particularly after refractive surgery. Corneal changes with accommodation occur more commonly in patients with keratoconus.<sup>14</sup> However, in the current study, involving normal corneas, there was no strong association between decreased corneal stiffness and increased corneal conformational changes with accommodation. Conformational changes may be useful as a risk factor for corneal ectasia in patients considering laser refractive surgery. Given the low incidence of post-refractive-surgery ectasia and the requirement for multiple tomographical assessments, assessing conformational changes may not be practical for preoperative refractive screening, and large numbers of patients would need to be assessed before this hypothesis could be tested.<sup>35</sup>

The ability to screen for ectasia risk using conformational changes with accommodation remains unknown as the subjects in the current study were all emmetropic and presumably at no risk of ectasia. Last, and perhaps more clinically relevant, would be the screening of patients with forme fruste, unilateral (in the uninvolved eye), or early keratoconus to detect those likely to develop keratoconus or progressive ectasia. If accommodative conformational changes could predict patients at high risk of

progression, it may assist decision-making for the necessity and timing of corneal collagen crosslinking. Serial tomography assessments, currently used to assess the criteria for crosslinking, can be expensive and time-consuming, leading to delays in treatment and deterioration in uncorrected visual acuity in some cases.

The current study demonstrates a baseline of statistically significant changes in central and peripheral corneal curvature up to 0.1 D, in young participants free from corneal pathology with ocular accommodation. However, the regions of change in each of these parameters were not well related to one another, and the changes were within the repeatability of the GALILEI G2 tomographer. Demographic and corneal biomechanical factors are also poor predictors of these changes. These findings support the growing body of evidence that suggests that corneal changes during accommodation have minimal impact on normal vision in humans and do not require routine clinical consideration. It was, however, possible to acquire high-quality scans from the GALILEI G2 tomographer with an alternative visual target by utilizing a beam splitter and a 3D-printed mount. This specific arrangement may have applications for future research studies related to accommodation, and it may be possible to modify other ophthalmic technologies in a similar manner.

## Acknowledgments

The authors thank Charles McGhee for his input and support. The authors also thank Simon Dean and Bruce Hadden for helpful discussion in preparing for the study.

Disclosure: **H.B. Wallace**, None; **J. Mckelvie**, None; **C.R. Green**, None; **S.L. Misra**, None

## References

1. Atchison DA, Smith G. *Optics of the human eye*. 1st ed. Oxford: Butterworth-Heinemann; 2000:64.
2. Rohen JW, Lütjen E, Bárány E. The relation between the ciliary muscle and the trabecular meshwork and its importance for the effect of miotics on aqueous outflow resistance. *Albrecht*

- von Graefes *Arch Klin Ophthalmol*. 1967;172:23–47.
3. Chu CHG, Zhou Y, Zheng Y, Kee CS. Bi-directional corneal accommodation in alert chicks with experimentally-induced astigmatism. *Vision Res*. 2014;98:26–34.
  4. Yasuda A, Yamaguchi T, Ohkoshi K. Corneal steepening during accommodation. *J Cataract Refract Surg*. 2004;30:1611–1612.
  5. Siso-Fuertes I, Dominguez-Vicent A, del Aguila-Carrasco A, Ferrer-Blasco T, Montes-Mico R. Corneal changes with accommodation using dual Scheimpflug photography. *J Cataract Refract Surg*. 2015;41:981–989.
  6. Ni Y, Liu X, Lin Y, Guo X, Wang X, Liu Y. Evaluation of corneal changes with accommodation in young and presbyopic populations using Pentacam High Resolution Scheimpflug system. *Clin Experiment Ophthalmol*. 2013;41:244–250.
  7. Kohlrausch F. Über die Messung des Radius der Vorderfläche der Hornhaut am lebenden Menschen. *Oken's Isis (Dresden)*. 1870;5:886–99.
  8. Fairmaid JA. The constancy of corneal curvature; an examination of corneal response to changes in accommodation and convergence. *Br J Physiol Opt*. 1959;16:2–23.
  9. Pierscionek BK, Popiolek-Masajada A, Kasprzak H. Corneal shape change during accommodation. *Eye*. 2001;15:766–769.
  10. Yasuda A, Yamaguchi T. Steepening of corneal curvature with contraction of the ciliary muscle. *J Cataract Refract Surg*. 2005;31:1177–1181.
  11. He JC, Gwiazda J, Thorn F, Held R, Huang W. Change in corneal shape and corneal wave-front aberrations with accommodation. *J Vis*. 2003;3:456–463.
  12. Bayramlar H, Sadigov F, Yildirim A. Effect of accommodation on corneal topography. *Cornea*. 2013;32:1251–1254.
  13. Read SA, Buehren T, Collins MJ. Influence of accommodation on the anterior and posterior cornea. *J Cataract Refract Surg*. 2007;33:1877–1885.
  14. Buehren T, Collins MJ, Loughridge J, Carney LG, Iskander DR. Corneal topography and accommodation. *Cornea*. 2003;22:311–316.
  15. Tarutta EP, Iomdina EN, Tarasova NA, Khodzhabekian NV. [On the contribution of cornea into accommodation of myopic eye]. *Vestn Oftalmol*. 2010;126:15–18.
  16. Stone J, Francis J. Practical optics of contact lenses, and aspects of contact lens design. In: Stone J, Phillips AJ, eds. *Contact Lenses: A Textbook for Practitioner and Student*. 2nd ed. London: Butterworths. 1980;91–140.
  17. Schachar RA, Tello C, Cudmore DR, Liebmann JM, Black TD, Ritch R. In vivo increase of the human lens equatorial diameter during accommodation. *Am J Physiol*. 1996;271:R670–R676.
  18. Ahearne M, Yang Y, Then KY, Liu KK. An indentation technique to characterize the mechanical and viscoelastic properties of human and porcine corneas. *Ann Biomed Eng*. 2007;35:1608–1616.
  19. Roberts CJ, Mahmoud AM, Bons JP, et al. Introduction of two novel stiffness parameters and interpretation of air puff-induced biomechanical deformation parameters with a dynamic Scheimpflug analyzer. *J Refract Surg*. 2017;33:266–273.
  20. Pelli DG, Robson JG, Wilkins A. The design of a new letter chart for measuring contrast sensitivity. *Clinical Vision Sciences*. 1988;2:187–199.
  21. Buehren T, Lee BJ, Collins MJ, Iskander DR. Ocular microfluctuations and videokeratoscopy. *Cornea*. 2002;21:346–351.
  22. Bland JM, Altman D. Statistical methods for assessing agreement between two methods of clinical measurement. *Lancet*. 1986;327:307–310.
  23. Bland JM, Altman DG. Measurement error and correlation coefficients. *BMJ*. 1996;313:41.
  24. Bland JM, Altman DG. Measuring agreement in method comparison studies. *Stat Methods Med Res*. 1999;8:135–160.
  25. Akima H. A method of bivariate interpolation and smooth surface fitting based on local procedures. *Commun ACM*. 1974;1:18–20.
  26. Newcombe RG. Two-sided confidence intervals for the single proportion: comparison of seven methods. *Stat Med*. 1998;17:857–872.
  27. Altıparmak Z, Yağcı R, Güler E, Arslanyılmaz Z, Canbal M, Hepşen İF. Repeatability and reproducibility of anterior segment measurements in normal eyes using dual scheimpflug analyzer. *Turk Oftalmoloji Dergisi*. 2015;45:243–248.
  28. Maurice DM. The cornea and sclera. *The Eye*. 1984;1:1–158.
  29. Andreassen TT, Simonsen AH, Oxlund H. Biomechanical properties of keratoconus and normal corneas. *Exp Eye Res*. 1980;31:435–441.
  30. Glasser A, Campbell MCW. Presbyopia and the optical changes in the human crystalline lens with age. *Vision Res*. 1998;38:209–229.
  31. Elsheikh A, Wang D, Brown M, Rama P, Campanelli M, Pye D. Assessment of corneal biomechanical properties and their variation with age. *Curr Eye Res*. 2007;32:11–19.

32. Strenk SA, Semmlow JL, Strenk LM, Munoz P, Gronlund-Jacob J, DeMarco JK. Age-related changes in human ciliary muscle and lens: a magnetic resonance imaging study. *Invest Ophthalmol Vis Sci.* 1999;40:1162–1169.
33. Tamm S, Tamm E, Rohen JW. Age-related changes of the human ciliary muscle. A quantitative morphometric study. *Mech Ageing Dev.* 1992;62:209–221.
34. Fincham EF. The accommodation reflex and its stimulus. *Br J Ophthalmol.* 1951;35:381.
35. Rad AS, Jabbarvand M, Saifi N. Progressive keratectasia after laser in situ keratomileusis. *J Refract Surg.* 2004;20:S718–S722.